forests

MDPI

Article

Identification, Evolution and Expression Analysis of GRF Family Reveals Their Involvement in Shoot Growth and Abiotic Stress Response in Moso Bamboo

Binao Zhou [1,2,3], Cheng Long [1,2,3], Wenjing Yao [1,2,3], Shuyan Lin [1,2,3] and Long Li [1,2,3,*]

[1] Co-Innovation Center for Sustainable Forestry in Southern China, Nanjing Forestry University, Nanjing 210037, China; bnzhou@njfu.edu.cn (B.Z.); cl13467235586@163.com (C.L.); yaowenjing@njfu.edu.cn (W.Y.); lrx@njfu.com.cn (S.L.)
[2] Bamboo Research Institute, Nanjing Forestry University, Nanjing 210037, China
[3] School of Life Science, Nanjing Forestry University, Nanjing 210037, China
* Correspondence: lilong1949@126.com

Abstract: Growth-regulating factors (GRFs) play an important role in regulating plant organ development, acting primarily as positive regulators of cell proliferation. However, research on the evolutionary history and expression patterns of the moso bamboo GRF family has been limited. In this study, a total of 24 GRFs have been identified in the Moso bamboo genome, and they have been categorized into four subfamilies. Estimation of the divergence time of paralogous gene pairs provided evidence supporting the significant contribution of recent whole-genome duplication events in the expansion of the GRF gene family. Sliding window analysis revealed that coding regions of a few *PheGRFs*, including the WRC and QLQ domains, may have undergone positive selection, possibly due to the redundant functions of paralogous genes. Coexpression network analysis further revealed the regulatory role of *miR396* and various *lncRNAs* in controlling PheGRF expression. Based on the analysis of tissue-specific expression patterns using transcriptome sequencing, qRT-PCR results, and in situ hybridization, it was observed that most GRFs, particularly *PheGRF6a* and *PheGRF9b*, exhibited high levels of accumulation in the moso bamboo shoot. This suggests that the involvement of most PheGRF genes may be crucial for the growth and development of the bamboo shoot. A yeast two-hybrid screening revealed interactions between PheGRF9b and several proteins associated with plant growth and development, including PH02Gene11097.t1 (GIF3), PH02Gene37618.t (Phytochrome B), and PH02Gene01921.t3 (WD40). Based on transcriptome expression analysis, it was observed that a substantial number of *PheGRFs* exhibited significant variations under cold or drought stress treatments, and most of these genes were found to be downregulated, suggesting their role as abiotic stress-responsive genes. Our findings offer new insights into the GRF family of moso bamboo and provide some experimental evidence to support further gene functional validation research of PheGRF.

Keywords: moso bamboo; GRF family; whole-genome duplication events; bamboo shoot

Citation: Zhou, B.; Long, C.; Yao, W.; Lin, S.; Li, L. Identification, Evolution and Expression Analysis of GRF Family Reveals Their Involvement in Shoot Growth and Abiotic Stress Response in Moso Bamboo. *Forests* **2023**, *14*, 2044. https://doi.org/10.3390/f14102044

Academic Editor: Tadeusz Malewski

Received: 11 August 2023
Revised: 20 September 2023
Accepted: 23 September 2023
Published: 12 October 2023

1. Introduction

Moso bamboo (*Phyllostachys edulis*) is a plant known for its abundant lignocellulosic resources with great ecological and economic value. Its bamboo shoots can be used as food, while the culms can be processed and applied to the industries of paper-making and timber production. Under optimal spring conditions, the bamboo shoots can grow up to 1 m in a mere 24 h, rapidly reaching a final height of 15–20 m within a span of one to two months. Owing to its incredible growth rate and exceptional strength, moso bamboo contributes an estimated 5 billion dollars in revenue, encompassing both the timber processing and food industries [1].

During the rapid growth period of moso bamboo shoots, internode elongation is influenced by the simultaneous processes of cell division and cell elongation [2]. The growth-regulating factor (GRF) family plays a crucial role in regulating plant development and responses to stress [3]. It contains the QLQ domain and the WRC domain in its N-terminal region [4]. The QLQ domain can form a transcription activator with the GRF-interacting factor (GIF), while the WRC domain binds to the promoters of downstream genes, and regulate their expression [5].

The first *GRF* gene studied was *OsGRF1*, which plays a critical role in regulating stem elongation induced by gibberellic acid [6]. Consequently, early research on GRFs primarily focused on their involvement in leaf development by regulating cell proliferation and cell size [7,8]. However, more evidence has revealed that GRFs also play significant roles in root development, the formation of floral organs and seeds, as well as plant longevity [2].

Accumulating studies have demonstrated that GRFs also play a significant role in responding to various abiotic or biotic stresses [9–12]. For instance, the expression of *HpGRF6* in pitaya exhibited an upregulated trend under drought conditions, while it was reduced when exposed to high temperature and NaCl stress [13]. Similarly, *AtGRF1* and *AtGRF3* were found to be significantly downregulated after a period of water withholding during drought stress [14]. Moreover, ChIP-seq analysis revealed that several defense- and stress-related genes were identified as target genes of AtGRF1 and AtGRF3, providing insights into their potential roles in mediating the balance between growth and defense responses and integrating environmental signals into developmental programs [15]. Additionally, AtGRF7 has been shown to directly target and suppress the transcription of *DREB2A* by binding to its promoter region. Several stress-related genes were significantly induced in the *grf7* mutant in comparison to the wild type, resulting in enhanced salt and drought tolerance in the mutant [16].

Recently, the GRF families in *Arabidopsis thaliana* [17], *Oryza sativa* [18], *Saccharum* [19], *Spirodela polyrhiza* [20], *Triticum aestivum* L. [21], *Zanthoxylum armatum* DC. [22], Lettuce [23], and *Medicago truncatula* [24] have been identified and extensively studied. Previous studies have reported on the moso bamboo GRF family; however, these studies were based on the first version of the genome sequencing data [25,26]. Unfortunately, the gene assembly in this version was only conducted at the scaffold level, which posed limitations in mapping the *GRF* genes to specific chromosomes. Additionally, these studies did not provide an explanation of the *GRF* genes' expansion in terms of evolutionary perspectives. Moreover, the expression profile of GRFs and their interactors in moso bamboo shoot was not analyzed previously. To fill this knowledge gap, a screening of *GRFs* was performed using the second version of the genome sequencing data [27]. We conducted a comprehensive analysis to investigate the evolutionary expansion of the *GRF* gene family and examined the expression patterns of these genes during the development of various bamboo organs. Additionally, we analyzed their response to different abiotic stresses. Moreover, we successfully identified proteins that interact with GRF during the bamboo shoots growth and development using yeast two-hybrid library screening. These findings will provide valuable insights for future investigations into the functional studies of PheGRFs.

2. Results

2.1. Identification and Classification of the PheGRF Gene Family

We obtained potential GRFs from the moso bamboo genome using a BLASTP algorithm-based search with known GRF proteins from *A. thaliana* and *O. sativa* as seed sequences. After confirming the QLQ and WRC domains occurring in the putative sequence using the Swiss-Model online tool, a total of 24 moso bamboo GRFs were identified.

In order to investigate the evolutionary relationship between moso bamboo GRFs and GRFs in other model plants such as *O. sativa*, *B. distachyon*, and *A. thaliana*, we constructed a phylogenetic tree based on the Maximum Likelihood method. The 24 identified PheGRFs were categorized into six functional groups, with seven proteins in group I, four in group III, four in group IV, and seven in group V (Figure 1A). In addition, the phylogenetic

tree constructed based on the 24 moso bamboo GRF members demonstrated consistent grouping results, further indicating the reliability of our grouping method. Furthermore, the phylogenetic analysis of GRFs in these four species revealed that PheGRFs showed more sequence similarity with OsGRFs and BdGRFs than with AtGRFs. For instance, subfamily IV and subfamily II only included members from Arabidopsis and did not include members from monocotyledonous plants.

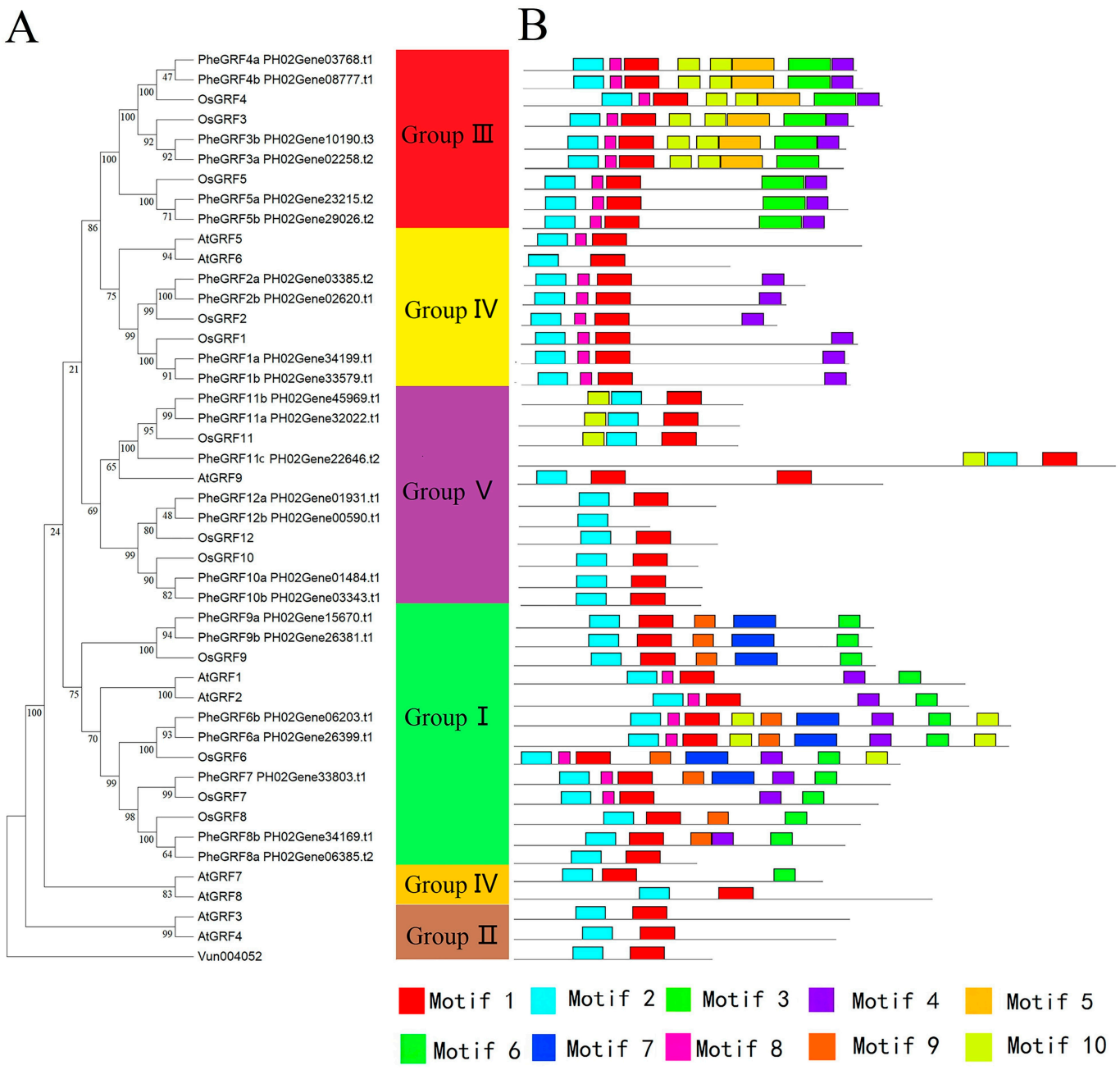

Figure 1. Phylogenetic analysis and motif compositions of the *PheGRF* family. (**A**) The phylogenetic tree illustrates the relationship among *GRF* members in *O. sativa*, *B. distachyon*, and *A. thaliana*, and moso bamboo. The most primitive *Vigna unguiculata GRF* was used as an outgroup. (**B**) The distribution of conserved motifs is shown within each group.

2.2. Characterization of the PheGRF Gene Family

To gain further insights into the protein sequence features of the PheGRFs, we examined the conserved motifs in the 24 PheGRFs using MEME and compared them with motifs

found in *O. sativa*, Brachypodium, and Arabidopsis (Figure 1B and Figure S1). Motifs 1 and 2 which represented the WRC and QLQ domains occurred in all members of GRFs. Motif 5 appeared only in III, while motifs 7 and 9 were found specifically in group I. Motifs 3, 4, and 6 appeared in groups I, III, and IV. Motif 8 appeared in groups III and IV. Motif 10 appeared in I, III, and V, and most members in group III harbored motif 10. Motif analysis indicated that there are significant differences in amino acid sequences between monocotyledonous plants and dicotyledonous plants within the same group. To take group IV as an example, all dicotyledonous amino acid sequences include motif 4, but not in *A. thaliana*.

Gene structural analysis of *PheGRFs* unveiled that genes in the same group exhibited similar intron lengths and numbers (Figure 2B). Except for *PheGRF11c* and *AtGRF5* who contained nine and three introns, respectively, the intron quantity of other members in the II, IV, and V is two. Except for *OsGRF6* whose intron number is two, the other members in the group I harbored three introns. The *AtGRF7* and *AtGRF8* in group IV contained two and five introns, respectively. The number of introns in group III ranged from two to four.

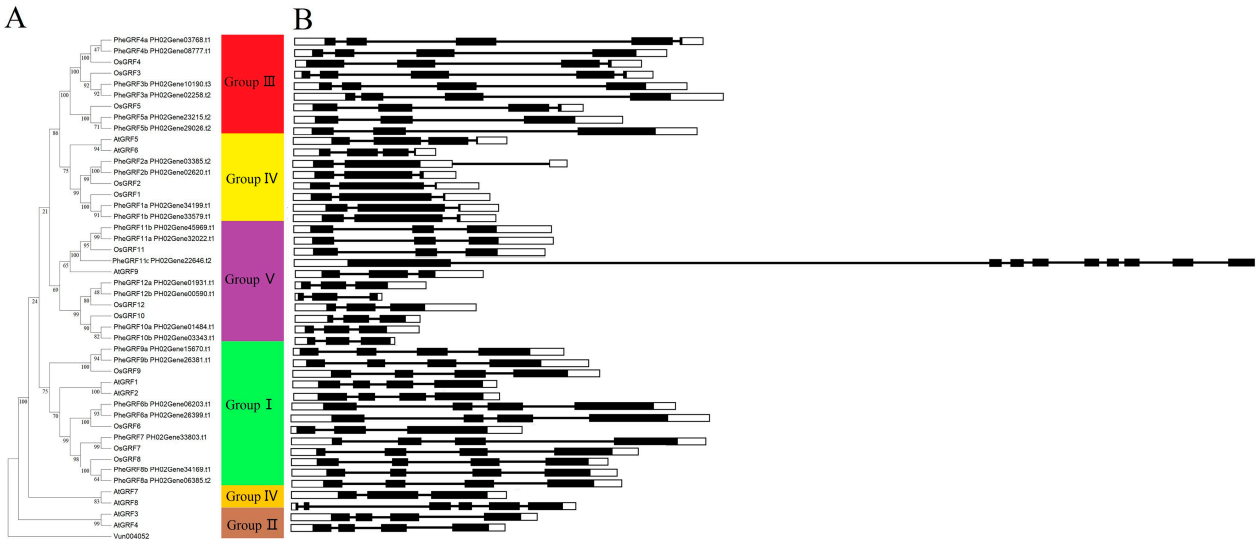

Figure 2. Phylogenetic tree and gene structure of the *PheGRF* family. (**A**) The phylogenetic tree illustrates the relationship among members of the *GRF* family. (**B**) The gene structure within each group is depicted.

Gene duplication events are essential for the generation of new functions and the expansion of gene families. In comparison to model plants like *O. sativa* and Arabidopsis, there is evident expansion in the PheGRF family. Therefore, we conducted an analysis to identify potential duplication events in the *PheGRFs*. As a result, 18 duplication gene pairs including 15 whole-genome duplication (WGD) pairs and three dispersed duplication (DD) pairs were found. Furthermore, all 15 identified WGD pairs were located in long fragment synteny blocks (Figure 3A). For instance, a significant number of synteny blocks were observed between chromosomes 3 and 17, which contained three paralogous gene pairs: *PheGRF1a-PheGRF1b*, *PheGRF4a-PheGRF4b*, and *PheGRF10a-PheGRF10b* (Figure 3B). Similar patterns were observed between chromosomes 23 and 24, which contained two paralogous gene pairs: *PheGRF3a-PheGRF3b* and *PheGRF12a-PheGRF12b*, respectively. These observations were also made for other chromosome pairs, whether they contained GRF paralogous pairs or not.

To investigate the selection pressure acting on moso bamboo *GRFs*, we computed the Ka/Ks values for each paralogous pair (Table S1). The Ka/Ks values of WGD-derived gene pairs were significantly higher than those of DD-derived gene pairs (Figure 3C), indicating that these genes have experienced stronger selection pressures. Notably, all gene pairs exhibited Ka/Ks values less than 1 (Figure 3D), suggesting the predominant role of purifying selection involved in shaping the evolution of moso bamboo. Furthermore, the

calculation of divergence time for the WGD pairs revealed that 10 out of 15 *PheGRF* gene pairs diverged approximately 6.5 to 13.5 million years ago, which aligns with the timeframe of the moso bamboo whole genome duplication event that occurred 7–12 million years ago, suggesting that the WGD played a critical role in the *PheGRF* expansion.

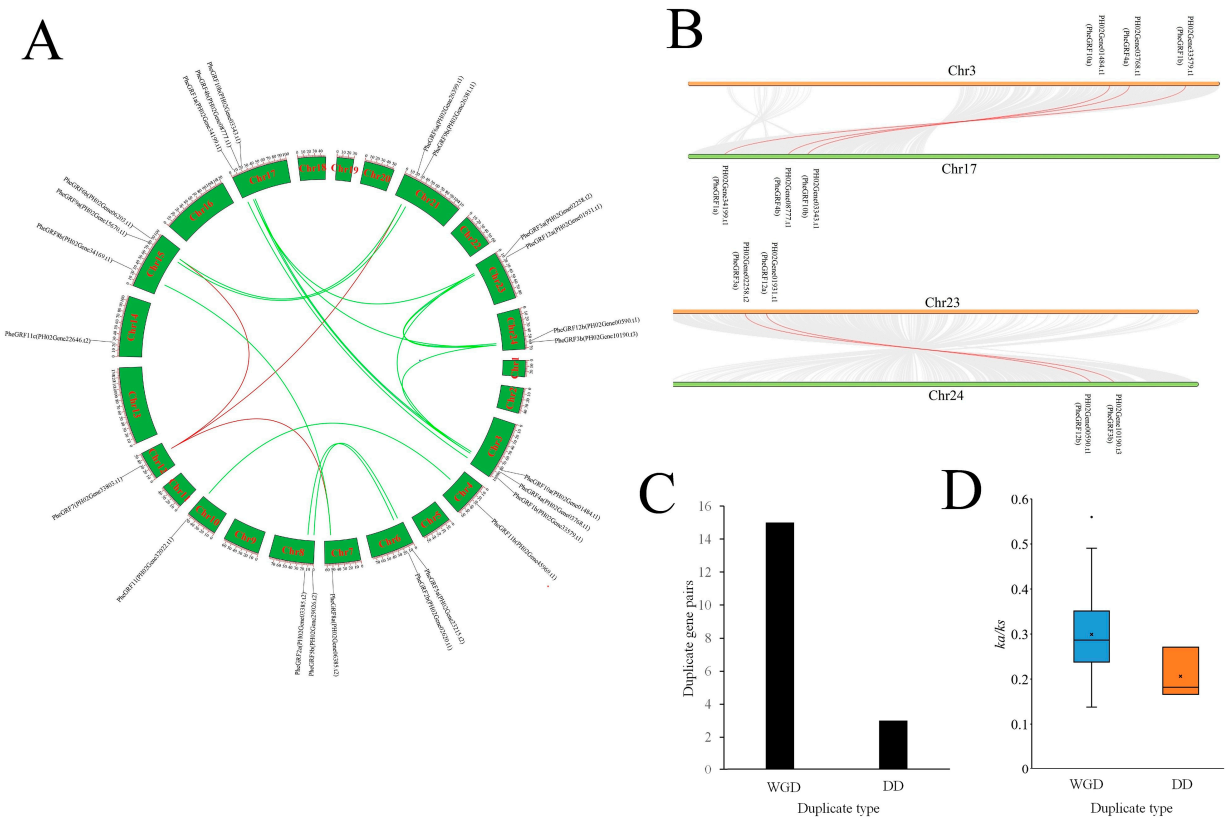

Figure 3. The expansion analysis of moso bamboo *GRFs*. (**A**) Syntenic relationships among *GRF* gene pairs. Gene pairs originating from whole-genome duplication (WGD) are connected by green lines, while dispersed pairs are connected by red lines. (**B**) An example of collinearity analysis between two moso bamboo chromosomes. The grey lines represent all the duplicated gene pairs, while the duplicated *PheGRFs* pairs are specifically connected by red lines. (**C**) The number of duplicate gene pairs of different duplication modes. (**D**) Comparison of *Ka/Ks* values between WGD and DD. WGD refers to whole-genome duplication, while DD represents dispersed duplication. The dots in box plot represent outliers.

We performed a sliding window analysis to estimate the evolutionary rate for each codon, taking into account that strong purifying selection can obscure positive selection at specific amino acid sites or regions (Figure 4). The results indicate that the majority of PheGRF pairs have undergone significant purifying selection, with an average Ka/Ks ratio of 0.15. For gene pairs in moso bamboo, most of the Ka/Ks ratios across the coding regions were less than 1. However, positive selection sites were identified in many coding regions, with the majority located in the non-conserved region. A few amino acid sites in conserved domains were also affected by positive selection, including four pairs of the WRC domain and four pairs of the QLQ domain. These results suggest that coding regions of *PheGRF*, including the WRC and QLQ domains, may undergo positive selection as a result of the potential redundancy in paralogous functions.

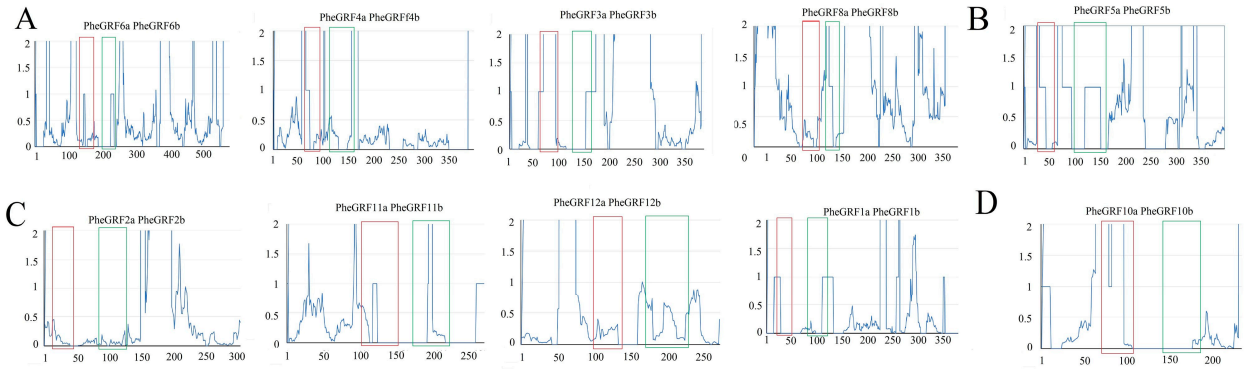

Figure 4. The sliding window of *PheGRF* paralogous genes. (**A**) Group I, (**B**) group III, (**C**) group IV, (**D**) group V. The red and green box indicated the WRC domain and QLQ domain, respectively.

2.3. Regulatory Network of PheGRF in Moso Bamboo

A large number of hormone response sites, meristem-related motifs, and transcription factor binding sites were found at the *PheGRF* candidate promoter regions (CPRs)(Figure 5). Fourteen *PheGRF* CPRs contained at least one gibberellin response site (such as P-box or GARE motifs). The MeJA and abscisic acid response sites were found in almost all *PheGRF* CPRs. Seventeen *PheGRF* CPRs contained the ARE-box motif, an anaerobic induction-related *cis*-element. Furthermore, it was observed that the WRE3 motif and LTR element, which are responsive to adversity, stress, and low temperature, were present in the majority of *PheGRF* CPRs. Additionally, it was found that 16 CPRs contained at least one meristem expression-related motif. This includes the CAT-box motif, which was present in 14 PheGRF CPRs, and the coexistence of the CCGTCC motif and CCGTCC-box in seven different GRF CPRs. These findings highlight that the regulation of PheGRFs is influenced by a variety of factors, including hormones and environmental cues. Furthermore, they emphasize the significance of PheGRFs in important cellular processes such as cell division and proliferation.

To better show the underlying relationship of *miRNAs*, *lncRNAs*, and *GRFs*, we created an interaction network on the basis of bamboo shoot growth and development-associated transcriptome sequencing data and degradome sequencing data which were published previously (Figure S3) [28,29]. In the network, a total of 10 *miRNAs* and 22 *lncRNAs* had a correlation with at least one *PheGRF* gene (Figure 6). The main hub *miRNA gma-miR396e* with the highest connecting times negatively correlated with the expression of *PheGRF5a*, *PheGRF5b*, *PheGRF6a*, *PheGRF6b*, etc. *LncRNA* target gene prediction based on position relationship and complementary sequence indicated that a total of 15 *GRF* genes may be regulated by *lncRNA*, and the most of them regulate the expression of *PheGRF11b*, among which the *lncRNA* regulating the expression of *PheGRF11b* is the most significant, two are positively correlated, and two are negatively correlated.

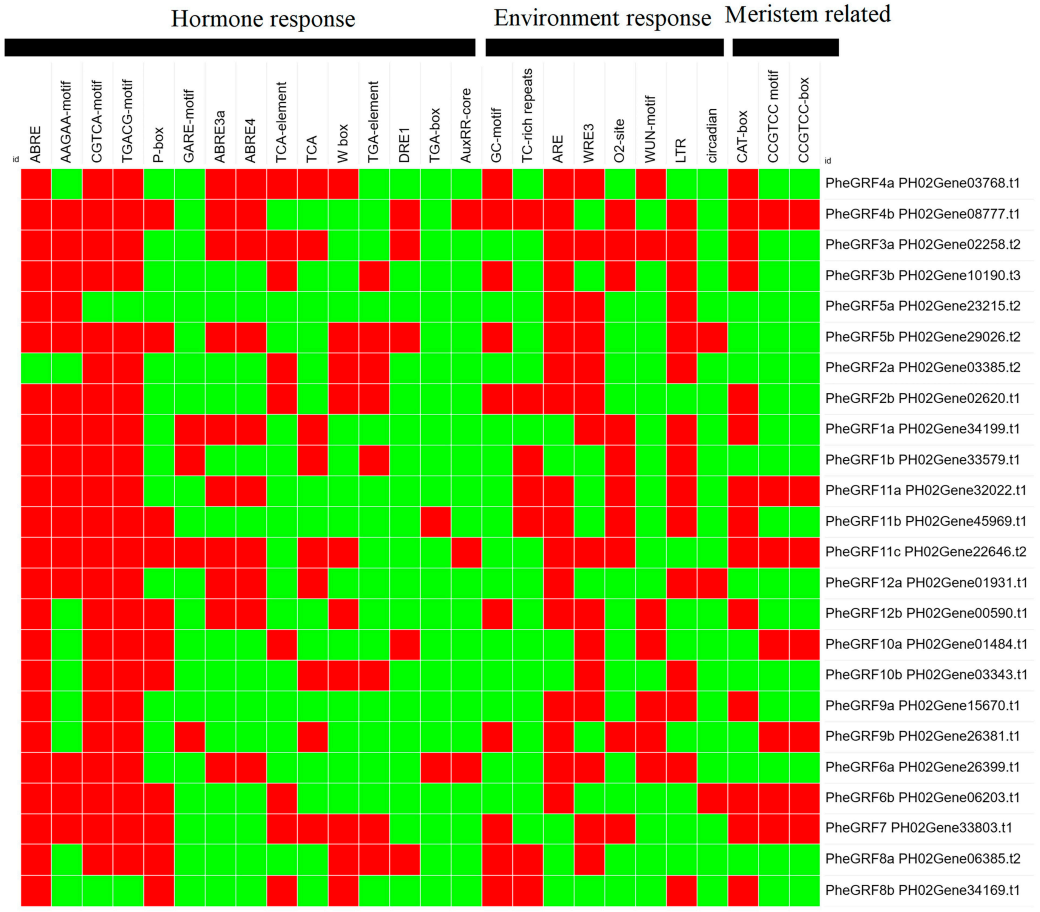

Figure 5. Analysis of *Cis*-acting elements on *PheGRF* promoters. Red indicates that the promoter contains this regulatory element, while green indicates that the regulatory element is not present in the promoter.

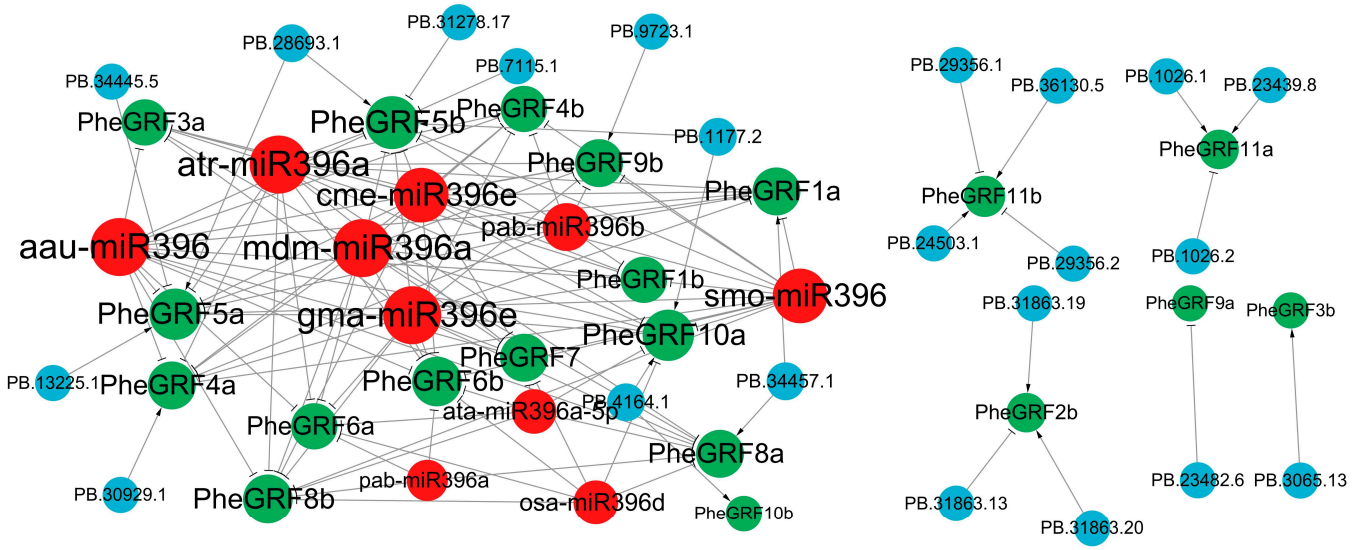

Figure 6. Predicted regulatory network of lncRNA, miRNA, and PheGRFs. Positive correlation is indicated by regular arrows, while negative correlation is indicated by a T-type arrow. Larger circles indicate genes with more connections. Within the network, red, blue, and green circles represent miRNAs, lncRNAs, and PheGRFs, respectively.

In order to identify proteins that potentially interact with PheGRF9b during moso bamboo shoot growth, we created a cDNA library specifically from bamboo shoots. Subsequently, we employed a yeast two-hybrid system to screen for interactors, with the goal of discovering potential chaperones for PheGRF9b. First, the yeast system was employed to analyze the auto-activation assays of PheGRF9a (Figure S4). The plasmids pGBKT7-PheGRF9a, pGAD7-T+pGBKT7-p53 (positive control), and pGBKT7 (negative control) were introduced into the yeast strain AH109, respectively. As shown in Figure 4, yeast cells containing the negative control plasmids pGBKT7 and pGBKT7-PheGRF9a did not grow on SD/-Trp/-Leu/-His/X-α-gal medium and did not produce a blue substrate. In contrast, the positive control pGAD7-T+pGBKT7-p53 grew well and produced a blue substrate. Therefore, PheGRF9a does not exhibit transcriptional self-activation activity in yeast cells. For the yeast double-hybrid library screening experiment, we utilized pGBKT7-PheGRF9b as the bait. Nine positive clones corresponding to five proteins were identified including PH02Gene11097.t1 (GIF3), PH02Gene28214.t1(MPK4), PH02Gene01921.t3(WD40), PH02Gene37618.t1 (Phytochrome B), and PH02Gene17719.t1(SAUR). Next, Y2H assay was employed to further confirm the interaction relationship (Figure 7). The pGBKT7-PheGRF9b and pGADT7-interactors plasmids were co-transformed into yeast AH109 cells, respectively, and subsequently selected on SD/-Trp/-Leu/-Ade/-His/X-α-Gal plates. After five days of cultivation, both the positive control and five experimental group displayed a blue color. These results indicate the presence of protein complexes during the growth of moso bamboo shoots.

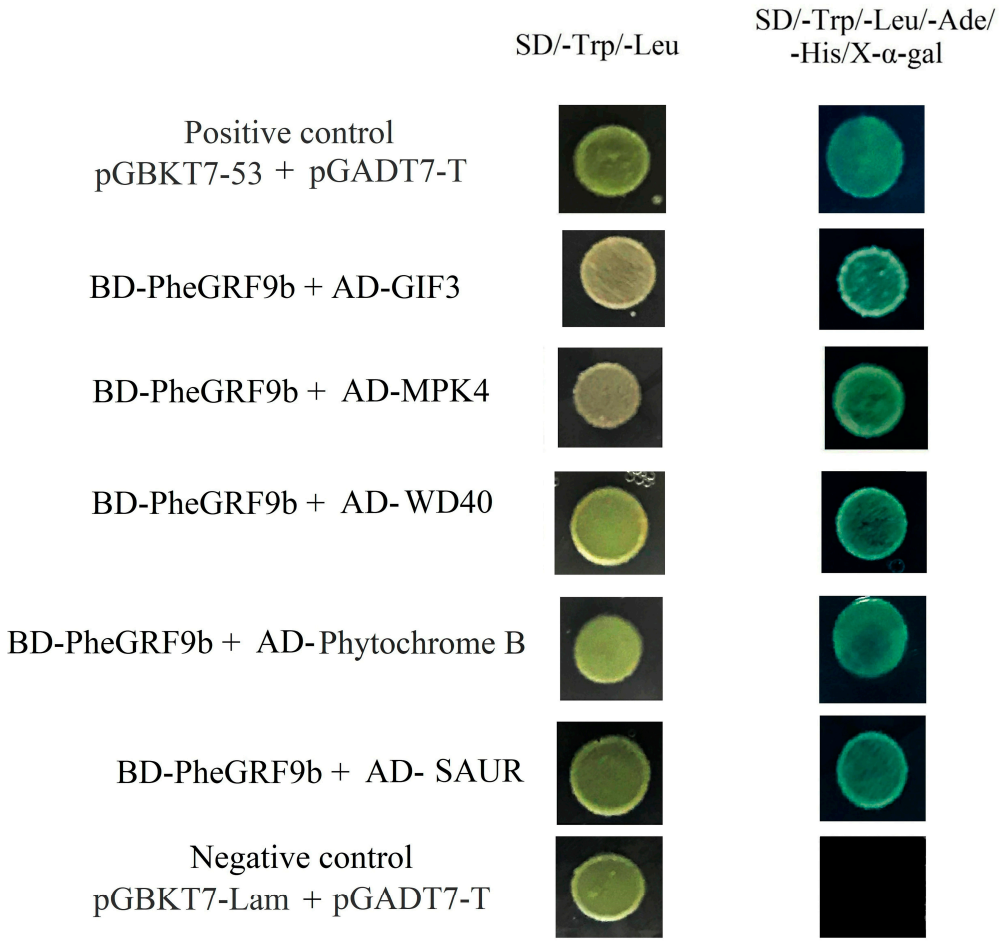

Figure 7. Identification of interactions between PheGRF9a and interactors in yeast. The yeast strains were cultured on Double Dropout Supplements (DDO)/−Trp/−Leu/X-α-gal and Quadruple Dropout Supplements (QDO)/−Trp/−Leu/−His/−Ade/X-α-gal/AbA media to assess the interactions.

2.4. Expression Profile of PheGRF Genes

The transcriptome data derived from 26 distinct bamboo tissues were utilized to examine the expression profiles of *PheGRFs* (Figure 8). Approximately half of the *PheGRFs*, including *PheGRF1a*, *2a*, *3a*, *4a*, *4b*, *5a*, *5b*, *6a*, *7*, *9a*, and *9b*, exhibited the highest expression levels in the 2 cm root which developed on the bottom of the bamboo shoot. Additionally, the majority of *PheGRFs* demonstrated relatively high expression levels in the 6.7 m high bamboo shoot, regardless of whether it originated from the top, middle, or lower portion. Since the rapid growth of bamboo shoots mainly relies on the elongation growth of internodes, we randomly selected five genes including *PheGRF3a*, *3b*, *5a*, *6a*, and *10b* and analyzed their expression patterns within a single internode during the rapid growth of bamboo shoots. Except for *PheGRF5a*, which shows similar expression levels in the basal and middle sections and lower expression in the top section, the other four genes all exhibit most expression levels in the basal section, followed by the middle section, and the lowest in the top section.

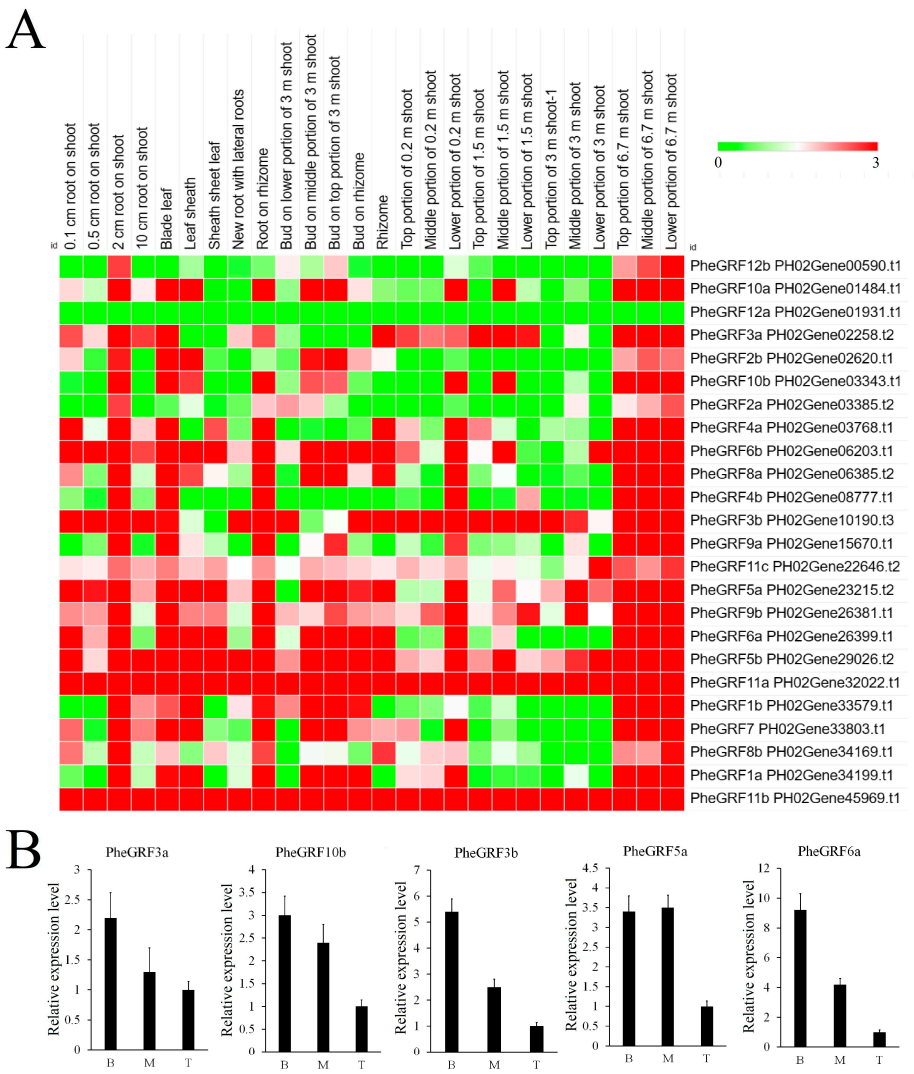

Figure 8. (**A**) Expression profiles of *GRFs* in different moso bamboo tissues. The color scale represents log2-transformed FPKM values. Red blocks with colors indicate high accumulation levels while green blocks indicate low accumulation levels. (**B**) Expression analysis of PheGRF in different part of a young single internode. The sample was taken from the 17th internode tissue of the shoot, starting from the base, at a height of 3.0 m. B, M, and T represent basal, middle, and top section of internode, respectively.

We selected *PheGRF6a* and *PheGRF9b*, which exhibited high expression levels in bamboo shoots, for further analysis using in situ hybridization (Figure 9). The results revealed that the two genes were highly expressed in both the ground tissues and vascular bundles of 6.7 m bamboo shoots. Particularly noteworthy is the high concentration of both genes in the phloem of the vascular bundles, indicating their active involvement in tissues undergoing cell division.

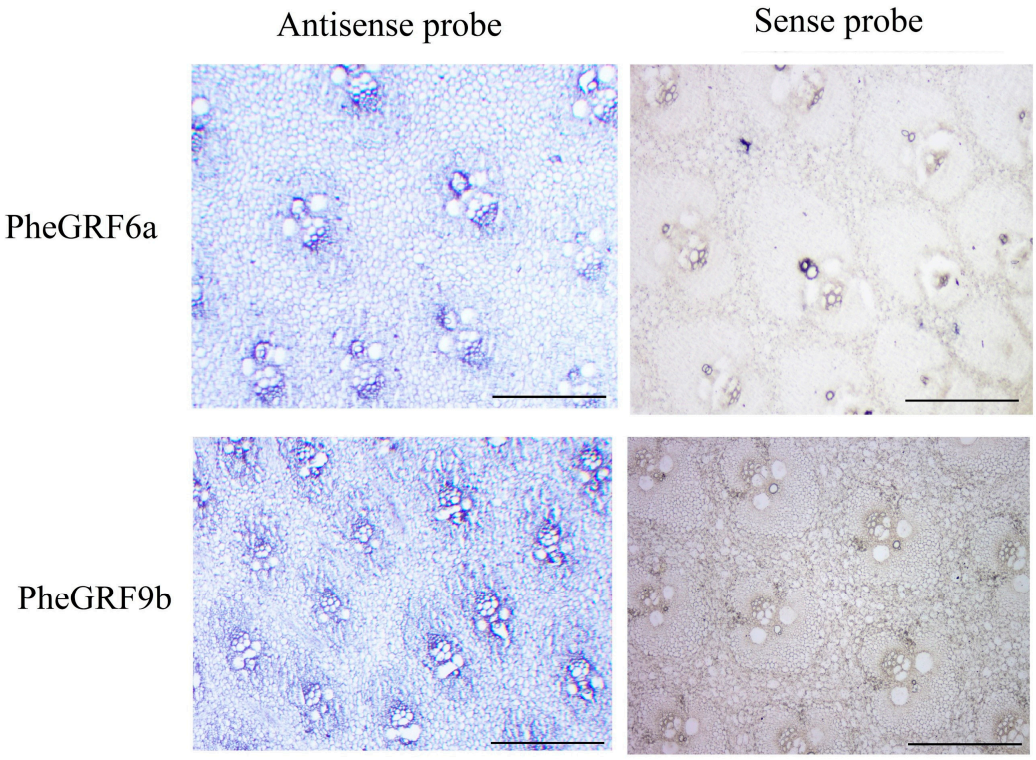

Figure 9. In situ hybridization of PheGRF6a and PheGRF9b in internode of winter moso bamboo shoots. Bars, 200 μm.

We further analyzed the expression patterns of 23 PheGRFs under drought or cold stress using transcriptome sequencing data (Figure 10A). A gene was considered upregulated or downregulated if it met the criteria of a False Discovery Rate (FDR) value ≤ 0.05 and a fold change ≥ 1. Among these genes, the majority exhibited varying degrees of downregulation under abiotic stress. However, the expression levels of *PheGRF2b*, *4a*, *6a*, *7*, *10b*, and *11b* gradually increased and reached their peak at 8 h under drought treatment. Furthermore, the expression of *PheGRF3a* and *12b* rapidly accumulated at 2 h and then decreased to low levels. Under cold treatment, the expression of *PheGRF1a*, *1b*, *3a*, *4a*, *4b*, *6a*, and *10a* peaked at 2 h, while *PheGRF9a* reached its peak expression at 8 h. To ensure the reliability of the transcriptomic data, we conducted qRT-PCR validation on five randomly selected genes. The qRT-PCR results revealed an average Pearson correlation coefficient of 0.77 between the qRT-PCR results and the expression levels obtained from the transcriptomic data (Figure 10B). This indicates that the qRT-PCR results generally reflect the transcriptomic data, although differences may be due to variations in the genetic background of the experimental seedlings.

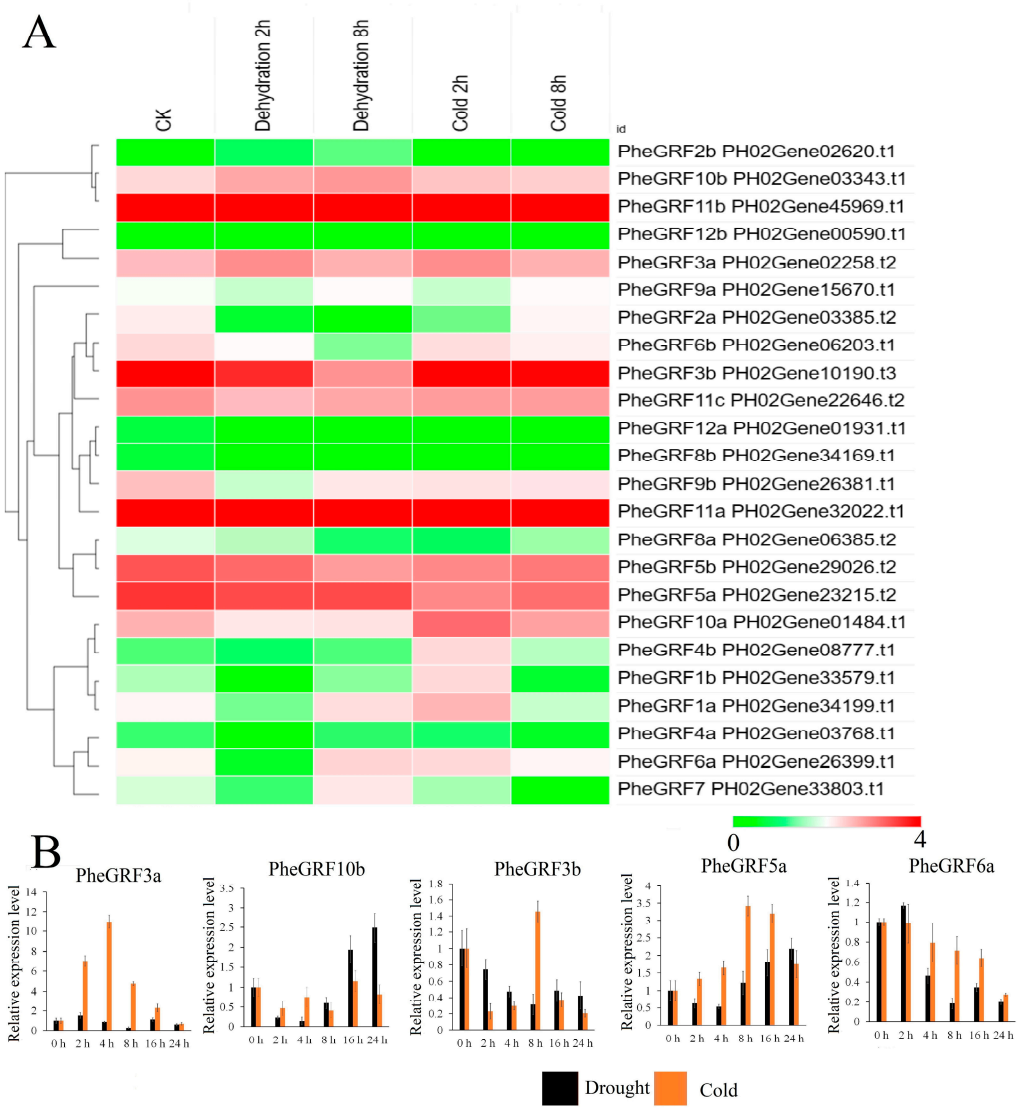

Figure 10. Expression patterns of *PheGRFs* under drought or cold treatments. (**A**) The expression profile of GRF genes based on transcriptomic data. The color scale represents log2 transformed FPKM values. Red blocks with colors indicate high accumulation levels while green blocks indicate low accumulation levels. (**B**) Validation of GRF transcriptomic data using qRT-PCR.

3. Discussion

In the moso bamboo genome, a total of 24 PheGRFs containing QLQ and WRC domains were identified, which is significantly higher compared to wheat (18), *Zea mays* (17), *O. sativa* (12), Arabidopsis (9), and Brachypodium (12) [21,30,31]. Despite having a genome size similar to *Z. mays* (2300 Mb) [32], moso bamboo (2021 Mb) has a smaller genome size than wheat (Triticeae) (17 Gb) [33], but larger than *A. thaliana* (164 Mb), *B. distachyon* (300 Mb), and *O. sativa* (441 Mb) [34–36]. The higher number of PheGRFs observed in moso bamboo suggests that it may be a result of gene duplication events. Gene duplication is a crucial process in the evolution of plants, particularly in relation to morphogenesis [37]. In plants, gene duplication can occur through WGD and single-gene duplication. WGD is believed to occur during speciation events, which leads to the emergence of multiple paralogs. Previous studies have indicated that moso bamboo originated from a tetraploid ancestor and underwent a long evolutionary process from tetraploidy to diploidy. The study suggests that the gene model sets of moso bamboo are similar to those of *O. sativa*, but moso bamboo carries two duplicates [27]. This phenomenon is consistently observed in the GRF family as well. In the moso bamboo genome, 15 pairs of *PheGRF* paralogous genes which

harbored in synteny blocks were identified. Additionally, the majority of divergence times among these *PheGRF* paralogous pairs occurred between 7–12 million years ago, which is consistent with the recent time of WGD occurrence. These findings strongly suggest that the expansion of *PheGRFs* is primarily driven by the whole-genome duplication event. A previous report suggested that only a subset of paralog pairs are maintained after WGD [38]. Through an analysis of the Arabidopsis genome, it was discovered that paralogs involved in signaling and transcriptional regulation are more likely to be retained. Furthermore, the complexity of plant morphology seemed to be positively correlated with the number of genes associated with transcriptional regulation [37,39]. Therefore, the expansion of the moso bamboo GRF transcription factor family through WGD has played a crucial role in shaping moso bamboo evolution and has contributed to the development of intricate morphological traits.

We calculated Ka/Ks values between *GRF* paralogous pairs to better understand the evolutionary patterns of them in moso bamboo. The results revealed that Ka/Ks values of all gene pairs were less than 1, indicating a significant occurrence of purifying selection during the evolutionary process of the PheGRF family [40]. Furthermore, the majority of the Ka/Ks values across the coding regions in each gene pair were less than 1. However, a few amino acid sites in conserved domains were also influenced by positive selection, including four pairs of WRC domains and four pairs of QLQ domains. These findings suggest that coding regions of *PheGRFs*, including the WRC and QLQ domains, may undergo positive selection as a result of the potential redundancy in paralogous function.

Previous studies have indicated that GRFs contribute to cell division and cell proliferation and meristem potential during the process of organogenesis [41]. Promoter analysis has provided valuable insights into the potential functions associated with meristem growth regulation and hormone-induced gene expression changes. Specifically, GA-responsive elements including GARE and P-box motifs were identified in the 14 PheGRFs' CPRs. Additionally, a significant number of stress-related hormone signal response regulatory elements were found in the moso bamboo GRF CPRs. For instance, MeJA-responsiveness and ABA-responsiveness elements were discovered in the *PheGRF* CPRs. A previous study based on in situ hybridization and yeast two-hybrid assay suggest that PheGRF4e could interact with PheIAA30, and act mainly on the root tip meristem and vascular bundle cells of developing bamboo shoots [42]. In *Spirodela polyrhiza*, abscisic acid (ABA) has been found to be highly effective in inducing the formation of turions. This process is accompanied by fluctuating expression levels of the *SpGRF* genes in their fronds [20]. These findings suggest that moso bamboo GRF has the potential to respond to hormone induction, including stress-related hormones, and play a role in the growth and development of multiple organs.

The analysis of cis-acting elements also uncovered the transcription and expression potential of *PheGRF* members under diverse stress conditions, including low temperature, drought, and anaerobic stress. Expression analysis confirmed the results obtained from promoter analysis, indicating that the majority of *PheGRFs* showed differential expression patterns under abiotic stress treatment, with most of them being downregulated. However, a small subset of *GRF* genes exhibited varying degrees of upregulated expression following exposure to the stress treatments. In Arabidopsis, GRFs interact with DELLAs and regulate growth under cold stress [43]. Under stress conditions, the overexpression of Arabidopsis AtGRF7 has been shown to enhance resistance to drought stress [16]. Additionally, AtGRF1 and AtGRF3 have been found to coordinate plant growth, defense signals, and stress responses [13]. These discoveries imply that PheGRFs could potentially play a role in biological processes associated with plant growth under different abiotic stress conditions.

Expression analysis of PheGRFs in different bamboo tissues indicated that different PheGRF genes exhibited expression specificity in different bamboo tissues, but most of them showed high accumulation levels in the 6.7 m high bamboo shoot, which corresponds to the fastest growth stage of the bamboo shoot [2]. In this study, we selected five GRF genes and investigated their expression levels in different parts of the same bamboo shoot internode. Through qRT-PCR analysis, it was found that the expression levels of these five

genes were lowest in the top part of the internode. Furthermore, previous studies have indicated that cells in the upper part of the bamboo shoot internode complete growth and development earlier and cease growth, while the basal part of the internode accumulates a large number of cells in the proliferation phase [44,45]. This suggests a close correlation between the expression of PheGRF genes and cell division, indicating that PheGRF may directly participate in cell division and growth in bamboo shoot internodes.

Based on the predicted co-expression network from degradation sequencing and bioinformatics analysis, it was discovered that *miRNA396* and *lncRNA* regulate the expression of PheGRF. In rice, the levels of most GRFs can be sensitively regulated by *miR396*, which responds to many developmental and environmental factors [46]. In culm growth, OsGRF7 causes a semidwarf and compact plant architecture with an increased culm wall thickness [47]. However, the role of mir396 in the internode elongation process of monocotyledonous plants is relatively understudied. We analyzed the sequencing data of bamboo shoot growth and development using degradation assays and found that mir396 plays a regulatory role in most members of the PheGRF family. Additionally, qRT-PCR quantification experiments revealed that PheGRF expression is highest in the basal cells of the internodes, suggesting a close correlation between PheGRF expression and cell division [44,45]. Based on these results and previous studies, we propose that the regulatory network formed by mir396-PheGRF plays an important role in the elongation of bamboo shoot internodes.

Currently, there are numerous studies focused on the regulatory role of lncRNAs in various plant organ development processes, such as flower, leaf [48], and root hair [49]. However, research on the regulation of stem growth and development by lncRNAs is still relatively limited. Through the construction of co-expression networks using LncTar 2.0 software and Pearson's correlation, we found that some lncRNAs may play a positive or negative regulatory role on the members of the GRF family during the growth and development of bamboo shoots, thus participating in the growth and development of bamboo shoots.

It is reported that the GRF can interact with the GIF family via the QLQ domain, resulting in the formation of an interaction complex that carries out transcriptional functions [43,50]. In our Y2H screening, we observed that PheGRF9b not only interacts with GIF3 but also interacts with other plant growth and development associated proteins, such as PH02Gene01921.t3 (WD40), PH02Gene37618.t (Phytochrome B), and PH02Gene17719.t1 (SAUR). SAURs are known to be involved in auxin signaling, Phytochrome Bs promote plant light responses through multiple pathways [51], and WD40 is involved in signal transduction, histone modification, cell cycle regulation, nuclear fusion, and RNA processing [52]. These findings suggest that PheGRFs may participate in various pathways by forming protein complexes with its interactors that are involved in diverse biological processes.

4. Methods

4.1. Identification of GRF Genes in Moso Bamboo Reference Genome

The peptide sequences of AtGRFs, OsGRFs, and BdGRFs were searched using the keyword "growth-regulating factor" in the Phytozome v12.1 database [53] (Table S2). These sequences were then used as queries to perform a BLASTp search against the moso bamboo annotation databases downloaded from GigaDB [26] (http://www.gigadb.org/dataset/100498, 10 August 2023). The search was conducted with a cutoff of e-value $\leq$ 0.0001. After a blast comparison, PROSITE (http://prosite.expasy.org, 10 August 2023) which is provided by the Swiss Institute of Bioinformatics was used to further check the QLQ and WRC domains, and the sequences that lacked these two domains were ruled out.

4.2. Multiple Sequence Alignment and Phylogenetic Analyses

The multiple sequence alignments were performed using the ClustalW program. The parameters used for running the CLUSTALW program were as follows: Scoring matrix for

amino acid sequences: BLOSUM62, gap open: 10, gap extension: 0.2, iteration: none [54]. Subsequently, the Maximum Likelihood (ML) tree was constructed using the IQ-Tree program [55], employing the best-fit tree model [55]. The JTT+R3 model was determined to be the most suitable model based on the Bayesian Information Criterion [55]. The bootstrap method was applied in a phylogeny test with 1000 replications. The generated results were then imported into FigTree v1.4.4 for further analysis and visualization [56].

4.3. Gene Structure, Motif, and Promoter Analysis

The GFF file containing the genomic annotations of PheGRFs was uploaded to the gene structure display server 2.0 to generate the gene structure diagrams [57]. The online program MEME was employed to identify motifs harbored in PheGRFs. MEME (Version: 5.5.1) was run locally with the following parameters: number of repetitions: any, maximum number of motifs: 8, and the optimum motif widths were constrained to between 25 and 200 residues [58]. The regulatory elements in the promoter region of *PheGRFs* (from −2000 bp to +1 bp) were analyzed using the PlantCARE online program.

4.4. Collinearity Analysis

Firstly, we conducted a comprehensive BLASTP analysis on all moso bamboo proteins, applying an E-value threshold of less than 1×10^{-6} and considering the top 5 matches. The GFF3 files contain the positional information of all genes, which were obtained from the moso bamboo annotation databases [26]. The obtained BLASTP results, along with gff3 files, were then utilized as the input files for the Multiple Collinearity Scan Toolkit [59]. This allowed us to identify duplication modes within the PheGRF gene family. The specific definition of the different duplication modes aligns with the previously described method [60]. Finally, we utilized the Circos (version: 0.69-9) software to visualize the results [61].

4.5. Estimation of Ka, Ks, and Divergence Time in Paralogous Pairs

Ka (nonsynonymous substitution), Ks (synonymous substitution), and the Ka/Ks value between the *GRF* paralogous pairs were determined using DnaSP 6.0 (DNA Sequence Polymorphism software 6.0) [62]. The Ka/Ks ratio provides insights into the evolutionary selection pressure on the duplicated genes: positive selection (Ka/Ks > 1), purifying selection (Ka/Ks < 1), and neutral selection (Ka/Ks = 1). The formula T = Ks/2λ was applied to estimate the divergence time of the duplication event, with a divergence rate λ of 6.5×10^{-9} in monocotyledons [63]. For identifying signals of positive selection in specific regions or amino sites, a sliding window analysis was performed using SWAKK [60].

4.6. In Situ Hybridization

The internodes, obtained from the middle section of the winter bamboo shoot with a height of approximately 10 cm, were fixed for 24 h in 4% paraformaldehyde solution. After dehydration using graded ethanol and vitrification with dimethylbenzene, the samples were embedded in paraffin. The paraffin blocks were then cut into sections that were 10 μm thick. Sections were treated with Proteinase K at a concentration of 1 μg/mL for 30 min at 37 °C. After the Proteinase K pre-treatment, the sections were incubated overnight at 43 °C with the RNA probes in a hybridization solution containing 40% deionized formamide. Following the hybridization, the sections were washed four times in 2XSSC (1XSSC: 150 mM sodium chloride and 15 mM sodium citrate) at 37 °C. Then, the slides were treated with RNase A at 37 °C for 30 min and washed with 0.1XSSC at 37 °C twice. To detect the hybridization signal, the DIG Nucleic Acid Detection Kit (Roche Biochemicals, Indianapolis, IN, USA) was used. The sections were incubated in the dark with the detection kit for 12 h, following the manufacturer's instructions. After the detection, the sections were dehydrated through an ethanol series (50% and 70% for 30 s each, and 99% for 1 min twice), air-dried, and mounted in Eukitt (O. Kindler, GmbH & Co., Freiburg, Germany). The hybridization signals were observed as a purple-red color by adding the substrates nitroblue tetrazolium/5-bromo-4-chloro-3-indolyl-phosphate (NBT/BCIP). The hybridization signals

were observed and photographed using an Olympus BX-51 microscope with a digital image acquisition system. The in situ probes were synthesized with digoxin labeling by Sangon company (Shanghai, China). The probe sequences were listed as follows: Antisense probe of PheGRF9b: 5′ AACGTGGGTTGTCGATTTGTAGAATTTAGCAGTGGAG 3′; Sense probe of PheGRF9b: 5′ TGGGAAAGCAGCAACCAGCAGAGCAATAAGAGC 3′; Antisense probe of PheGRF6a: 5′ TTGCTTCTCCCTGGCTAACTTCATCTTTATTTG 3′; Sense probe of PheGRF6a: CTTCCACATCTCCCATCCACGAGAAGCTAATG.

4.7. Yeast Two-Hybrid Assays

The complete open reading frame (ORF) of *PheGRF9b* was cloned using the following primers: forward, 5′-ATGTTTGCTGAGTTCTCTGCTGC-3′; reverse, 5′-CTACATTTCAT GGTCCTCGAGATTC-3′. TIANGEN DNA Polymerase (TIANGEN biological company, China) was used to amplify the *PheGRF9b* gene. The PCR parameters were 94 °C for 5 min, followed by 28 cycles of 94 °C for 30 s, 61 °C for 1 min, and 72 °C for 1 min. The PCR products were cloned into pGEM-T Easy (Promega, USA) after gel extraction. The target fragment in the clone was digested with *EcoR* I and *BamH* I and then introduced into the pGBKT7 bait vector. The constructed plasmid was confirmed by the chain-termination method on an ABI 3100 automated sequencer (USA).

For self-activation assays, the recombinant plasmid pGBKT7-PheGRF9b was transformed into AH109 yeast cells. The transformed yeast cells were evenly spread on SD/-Trp agar medium and incubated for 2–3 days. Then, they were inoculated onto selective media SD/-Trp, and SD/-Trp/-Leu/-His/X-α-gal. After inverting the plates, they were incubated at 30 °C for 3–4 days, and the growth status was observed and recorded. pGBKT7-p53 and pGADT7-T were co-transformed as positive controls, pGBKT7 empty vector was transformed as a negative control.

The moso bamboo cDNA library for Y2H experiments was constructed by OE BioTech (Shanghai, China) using cDNA synthesized from the mRNA of shoots at different developmental stages and cloned into the prey vector pGADT7 [28]. The pGBKT7-PheGRF9b was then used for Y2H screening of the pGADT7-based cDNA library. Y2H experiments were conducted using the Matchmaker GAL4 two-hybrid systems (TaKaRa, Kyoto, Japan). The putative PheGRF9b-interacting clones were identified on an SD/-Ade/-His/-Leu/-Trp/X-α-Gal medium and further characterized and sequenced. Negative controls included cotransformants containing pGBKT7-Lam and pGADT7-T, while the positive control included cotransformants containing pGBKT7-53 and pGADT7-T.

4.8. Transcriptome Data Analysis

The transcriptome data of PheGRFs from various bamboo tissues, bamboo shoots at different growth stages, and bamboo seedlings under drought or cold stresses have previously been generated and processed (PRJNA535488, PRJNA604634, PRJNA914504, PRJNA820321, SRR13986970) [64]. The expression level of PheGRFs was quantified as fragments per kilobase of exon model per million mapped reads (FPKM). The heatmap was visulized using Morpheus (http://software.broadinstitute.org/morpheus/, 10 August 2023).

4.9. qRT-PCR Analysis

The experimental treatments of abiotic stresses and sample collection for the bamboo were conducted following the methods previously reported to ensure consistency [43]. Leaves detached from three-week-old moso bamboo plants with similar growth status were used for the experiment. Dehydration treatment involved placing the whole leaves on dry filter paper at room temperature (20 °C and 50% humidity). For cold treatment, the leaves were placed in a chamber set to 0 °C without light. Bamboo tissues were collected at 2 h and 8 h after each treatment. Five individuals that showed similar growth patterns were pooled for each sample and three biological repeats were conducted for each sample.

Previous studies have demonstrated that the 17th internode from the base to the top of moso bamboo shoots exhibits the most consistent growth and development [45].

Consequently, samples were obtained from this specific internode of 3 m tall bamboo shoots for subsequent qRT-PCR expression analysis. The samples were further divided into upper, middle, and lower sections. To ensure representative samples, three individuals displaying similar growth patterns were pooled for each section, and three biological replicates were performed for each sample.

Total RNA was extracted from the frozen leaves using the RNA Easy Fast kit (DP452, TIANGEN, Beijing, China) following the manufacturer's instructions. First-strand cDNA synthesis was performed using the PrimeScriptTM RT reagent kit (TaKaRa, Kyoto, Japan). Quantitative real-time PCR (qRT-PCR) reactions were conducted using the SYBR™ Green Premix Pro Taq HS qPCR kit (Accurate Biology, Hunan, China) on an ABI stepone (Thermo fisher, Waltham, MA, USA). Gene primers were designed using Oligo 7 software (Table S3). The tonoplast intrinsic protein 41 (TIP41) was used as an internal reference gene. The relative expression levels of each gene were calculated using the $2^{-\triangle\triangle Ct}$ method.

4.10. lncRNA Identification

The identification of lncRNAs is based on previously published Pacific Biosciences Single-molecule long-read Sequencing data [28]. Moso bamboo lncRNAs were predicted using Transdecoder v3.0.1 from all previously sequenced PacBio isoforms. These isoforms were then filtered based on open reading frames (ORFs) longer than 100 amino acids [28]. To eliminate transcripts that are similar to known protein-coding genes, the lncRNAs that aligned with proteins from *Arabidopsis thaliana*, rice, and soybean in the Swiss-Prot database were removed (with an E-value $\leq 1 \times 10^{-10}$). Two methods were employed to predict the target genes. The first method involved the regulation of neighboring genes by *lncRNAs*. We defined differentially expressed lncRNAs and mRNAs within each 100 kbp range on the chromosome, based on their positional relationship. The second method involved the interaction between *lncRNAs* and mRNAs through complementary base pairing. We utilized the LncTar 2.0 tool to predict the target genes for the lncRNAs [65].

4.11. Degradome Sequencing and Target Gene of miRNA Identification

The degradation group sequencing library was prepared by combining equal amounts of total RNA from bamboo shoots at different underground growth stages [29]. The captured mRNA was ligated with 5′ adaptor primers, and then supplemented with KAPA Pure Beads. Reverse transcription was performed using reverse transcriptase (m0368; New England Biolabs, Ipswich, MA, United States). The degradation group sequencing library was prepared and single-ended sequenced using an NEBNext Ultra II RNA Library Prep Kit (e7770; New England Biolabs), and an Illumina HiSeq 2,500, respectively.

The Cleaveland 4.0 algorithm was used to predict the target genes [66], while oligomap (http://github.com/zavolanlab/oligomap, 10 August 2023) was employed to accurately match the mRNAs from different species to the moso bamboo degradation group sequence. To obtain effective data, redundant sequences were removed using the norm reads per million (NRPM) method. The mirU tool was utilized to retrieve all sequences that matched the target genes in the miRNA library [67], and the plant miRNA/target pairing standard was used to score the target genes. The number of unique genes and the mapping ratio between the degradation group fragments and ideal mRNA were then calculated to evaluate the quality of the degradation group sequencing.

4.12. Regulation Network Construction

The expression levels of lncRNAs that regulate PheGRF were retrieved from transcriptomic data of different tissues, along with the expression levels of PheGRF. The Pearson correlation coefficient between the lncRNA expression levels and PheGRF expression levels was calculated using Excel. Only the absolute values of Pearson correlation coefficients greater than 0.3 were retained for constructing the co-expression network. Coefficients greater than 0.3 are considered as positive regulation, while those less than −0.3 are considered as negative regulation. Since the regulatory relationship between miRNA and PheGRF

target genes is inferred from degradation data and is based on the widely recognized mechanism of miRNA action, which involves negative regulation, the regulatory relationship between miRNA and PheGRF is considered as negative regulation in the current study. The obtained regulatory relationship between lncRNAs and PheGRF, as well as the regulatory relationship between miRNA and PheGRF, were inputted into Cytoscape 3.7.0 software in the form of an Excel table to generate a co-expression network graph. Positive regulatory relationships are represented by arrows, while negative regulatory relationships are represented by T-arrows. The size of the circles is adjusted based on the number of gene connections.

5. Conclusions

Here, 24 GRFs were identified in moso bamboo genome. During the evolution of PheGRF genes, whole-genome duplication events have played a significant role. Expression analysis has indicated that PheGRFs are responsive to cold and drought stress and are involved in the growth and development of bamboo shoots. Coexpression network analysis and the yeast two-hybrid system have unveiled a complex regulatory network in which PheGRFs participate. These findings will offer valuable insights for future investigations into the functional studies of PheGRFs.

Supplementary Materials: The following supporting information can be downloaded at: https://www.mdpi.com/article/10.3390/f14102044/s1. Figure S1: The conserved motif identified in the moso bamboo GRF family. Figure S2: A neighbor-joining tree was constructed based on the alignment of full-length amino acid sequences of PheGRF protein. Figure S3: Splicing sites prediction based on degradation group sequencing. Figure S4: PheGRF9a self-transcription activation assay. Table S1: The Ka/Ks ratio of moso bamboo GRF gene pairs. Table S2: The accession numbers of the GRFs from each species. Table S3. Primers used for qRT-PCR.

Author Contributions: Conceptualization and supervision, B.Z.; funding acquisition, L.L. and S.L.; methodology and formal analyses, C.L. and W.Y.; writing—original draft preparation, B.Z. and L.L.; writing—review and editing, S.L.; resources and data curation, B.Z. and C.L. All authors have read and agreed to the published version of the manuscript.

Funding: This work was supported by the National Science Foundation of China (32201643) to L.L; National Key Research & Development Program of China (2021YFD2200503) to S.L.; the National Science Foundation of China (32001292) to W.Y.

Institutional Review Board Statement: Not applicable.

Informed Consent Statement: Not applicable.

Data Availability Statement: Not applicable.

Conflicts of Interest: The authors declare no conflict of interest.

References

1. Lobovikov, M.; Paudel, S.; Piazza, M.; Ren, H.; Wu, J. *World Bamboo Resources: A Thematic Study Prepared in the Framework of the Global Forest Resources Assessment 2005*; Non-Wood Forest Products (FAO): Rome, Italy, 2007.
2. Li, L.; Cheng, Z.C.; Ma, Y.J.; Bai, Q.S.; Li, X.Y.; Cao, Z.H.; Wu, Z.N.; Gao, J. The association of hormone signaling, transcription and anatomy during shoot growth in Moso bamboo. *Plant Biotechnol. J.* **2018**, *16*, 72–85. [CrossRef] [PubMed]
3. Liu, Y.; Guo, P.; Wang, J.; Xu, Z.Y. Growth-regulating factors: Conserved and divergent roles in plant growth and development and potential value for crop improvement. *Plant J.* **2023**, *113*, 1122–1145. [CrossRef] [PubMed]
4. Fonini, L.S.; Lazzarotto, F.; Barros, P.M.; Cabreira-Cagliari, C.; Martins, M.A.; Saibo, N.J.; Turchetto-Zolet, A.C.; Margis-Pinheiro, M. Molecular evolution and diversification of the GRF transcription factor family. *Genet Mol. Biol.* **2020**, *43*, 20200080. [CrossRef] [PubMed]
5. Bull, T.; Debernardi, J.; Reeves, M.; Hill, T.; Bertier, L.; Van Deynze, A.; Michelmore, R. GRF-GIF chimeric proteins enhance in vitro regeneration and Agrobacterium-mediated transformation efficiencies of lettuce (Lactuca spp.). *Plant Cell Rep.* **2023**, *42*, 629–643. [CrossRef] [PubMed]
6. van der Knaap, E.; Kim, J.H.; Kende, H. A novel gibberellin-induced gene from rice and its potential regulatory role in stem growth. *Plant Physiol.* **2000**, *122*, 695–704. [CrossRef]

7. Vercruysse, J.; Baekelandt, A.; Gonzalez, N.; Inzé, D. Molecular networks regulating cell division during Arabidopsis leaf growth. *J. Exp. Bot.* **2020**, *71*, 2365–2378. [CrossRef]
8. Wu, W.; Li, J.; Wang, Q.; Lv, K.; Du, K.; Zhang, W.; Li, Q.; Kang, X.; Wei, H. Growth-regulating factor 5 (GRF5)-mediated gene regulatory network promotes leaf growth and expansion in poplar. *New Phytol.* **2021**, *230*, 612–628. [CrossRef]
9. Zhang, Y.; Xiao, T.; Yi, F.; Yu, J. SimiR396d targets SiGRF1 to regulate drought tolerance and root growth in foxtail millet. *Plant Sci.* **2023**, *326*, 111492. [CrossRef]
10. Wang, P.; Xiao, Y.; Yan, M.; Yan, Y.; Lei, X.; Di, P.; Wang, Y. Whole-genome identification and expression profiling of growth-regulating factor (GRF) and GRF-interacting factor (GIF) gene families in Panax ginseng. *BMC Genom.* **2023**, *24*, 334. [CrossRef]
11. Shahan, R. The Cold Never Bothered Me Anyway: DELLA-Interacting GROWTH REGULATING FACTORS Mediate Plant Growth in Cold Stress. *Plant C.* **2020**, *32*, 797–798. [CrossRef]
12. Hu, Q.; Jiang, B.; Wang, L.; Song, Y.; Tang, X.; Zhao, Y.; Fan, X.; Gu, Y.; Zheng, Q.; Cheng, J.; et al. Genome-wide analysis of growth-regulating factor genes in grape (Vitis vinifera L.): Identification, characterization and their responsive expression to osmotic stress. *Plant Cell Rep.* **2023**, *42*, 107–121. [CrossRef]
13. Li, A.L.; Wen, Z.; Yang, K.; Wen, X.P. Conserved miR396b-GRF regulation is involved in abiotic stress responses in Pitaya (Hylocereus polyrhizus). *J. Mol. Sci.* **2019**, *20*, 2501. [CrossRef] [PubMed]
14. Casadevall, R.; Rodriguez, R.E.; Debernardi, J.M.; Palatnik, J.F.; Casati, P. Repression of Growth Regulating Factors by the MicroRNA396 inhibits cell proliferation by UV-B radiation in Arabidopsis leaves. *Plant C.* **2013**, *25*, 3570–3583. [CrossRef] [PubMed]
15. Piya, S.; Liu, J.; Burch-Smith, T.; Baum, T.J.; Hewezi, T. A role for Arabidopsis growth-regulating factors 1 and 3 in growth-stress antagonism. *J. Exp. Bot.* **2020**, *71*, 1402–1417. [CrossRef] [PubMed]
16. Kim, J.S.; Mizoi, J.; Kidokoro, S.; Maruyama, K.; Nakajima, J.; Nakashima, K.; Mitsuda, N.; Takiguchi, Y.; Ohme-Takagi, M.; Kondou, Y.; et al. Arabidopsis growth-regulating factor7 functions as a transcriptional repressor of abscisic acid- and osmotic stress-responsive genes, including DREB2A. *Plant C.* **2012**, *24*, 3393–3405. [CrossRef] [PubMed]
17. Kim, J.H.; Choi, D.; Kende, H. The AtGRF family of putative transcription factors is involved in leaf and cotyledon growth in Arabidopsis. *Plant J.* **2010**, *36*, 94–104. [CrossRef]
18. Choi, D.; Kim, J.H.; Kende, H. (Whole genome analysis of the OsGRF gene family encoding plant-specific putative transcription activators in rice (Oryza sativa L.). *Plant Cell Physiol.* **2004**, *45*, 897–904. [CrossRef]
19. Wu, Z.; Chen, X.; Fu, D.; Zeng, Q.; Gao, X.; Zhang, N.; Wu, J. Genome-wide characterization and expression analysis of the growth-regulating factor family in Saccharum. *BMC Plant Biol.* **2022**, *22*, 510. [CrossRef]
20. Li, G.; Chen, Y.; Zhao, X.; Yang, J.; Wang, X.; Li, X.; Hu, S.; Hou, H. Genome-wide analysis of the Growth-Regulating Factor (GRF) family in aquatic plants and their Rroles in the ABA-induced turion formation of Spirodela polyrhiza. *Int. J. Mol. Sci.* **2022**, *23*, 10485. [CrossRef]
21. Zan, T.; Zhang, L.; Xie, T.; Li, L. Genome-wide identification and analysis of the Growth-Regulating Factor (GRF) gene family and GRF-interacting factor family in Triticum aestivum L. *Biochem. Genet.* **2020**, *58*, 705–724. [CrossRef]
22. Huang, Y.; Chen, J.; Li, J.; Li, Y.; Zeng, X. Genome-wide identification and analysis of the Growth-Regulating Factor family in Zanthoxylum armatum DC and functional analysis of ZaGRF6 in leaf size and longevity regulation. *Int. J. Mol. Sci.* **2022**, *23*, 9043. [CrossRef] [PubMed]
23. Zhang, B.; Tong, Y.; Luo, K.; Zhai, Z.; Liu, X.; Shi, Z.; Zhang, D.; Li, D. Identification of GROWTH-REGULATING FACTOR transcription factors in lettuce (Lactuca sativa) genome and functional analysis of LsaGRF5 in leaf size regulation. *BMC Plant Biology.* **2022**, *21*, 485. [CrossRef] [PubMed]
24. Li, H.; Qiu, T.T.; Zhou, Z.S.; Kang, L.Q.; Chen, R.R.; Zeng, L.M.; Yu, H.Y.; Wang, Y.H.; Song, J.B. Genome-wide analysis of the Growth-Regulating Factor family in Medicago truncatula. *J. Plant Growth Regul.* **2022**, *23*, 6905. [CrossRef]
25. Shi, Y.; Liu, H.; Gao, Y.; Wang, Y.; Wu, M.; Xiang, Y. Genome-wide identification of growth-regulating factors in moso bamboo (Phyllostachys edulis): In silico and experimental analyses. *PeerJ.* **2019**, *12*, e7510. [CrossRef]
26. Peng, Z.H.; Lu, Y.; Li, L.B.; Zhao, Q.; Feng, Q. The draft genome of the fast-growing non-timber forest species Moso bamboo (Phyllostachys heterocycla). *Nat. Gene* **2013**, *45*, 456–461. [CrossRef] [PubMed]
27. Zhao, H.; Gao, Z.; Wang, L.; Wang, J.; Wang, S.; Fei, B.; Chen, C.; Shi, C.; Liu, X.; Zhang, H.; et al. Chromosome-level reference genome and alternative splicing atlas of moso bamboo (Phyllostachys edulis). *Gigascience* **2018**, *7*, giy115. [CrossRef]
28. Li, L.; Shi, Q.; Jia, Y.; Deng, P.; Gao, J. Transcriptome and anatomical comparisons reveal the specific characteristics and genes involved in distinct types of growing culms. *Ind. Crops Prod.* **2021**, *171*, 113865. [CrossRef]
29. Li, Y.; Zhang, D.; Zhang, S.; Lou, Y.; An, X.; Jiang, Z.; Gao, Z. Transcriptome and miRNAome analysis reveals components regulating tissue differentiation of bamboo shoots. *Plant Physiol.* **2022**, *188*, 2182–2198. [CrossRef]
30. Qin, L.; Chen, H.; Wu, Q.; Wang, X. Identification and exploration of the GRF and GIF families in maize and foxtail millet. *Physiol. Mol. Biol. Plants.* **2022**, *28*, 1717–1735. [CrossRef]
31. Wang, W.; Cheng, M.; Wei, X.; Wang, R.; Fan, F.; Wang, Z.; Tian, Z.; Li, S.; Yuan, H. Comprehensive evolutionary analysis of growth-regulating factor gene family revealing the potential molecular basis under multiple hormonal stress in Gramineae crops. *Front. Plant Sci.* **2023**, *14*, 1174955. [CrossRef]
32. Duvick, J.; Fu, A.; Muppirala, U.; Sabharval, M.; Wilkerson, M.D.; Lawrence, C.J.; Lushbough, C.; Brendel, V. PlantGDB: A resource for comparative plant genomics. *Nucl. Acids Res.* **2008**, *36*, D959. [CrossRef] [PubMed]

33. International Wheat Genome Sequencing Consortium. A chromosomebased draft sequence of the hexaploid bread wheat (Triticum aestivum) genome. *Science* **2014**, *345*, 1251788. [CrossRef] [PubMed]
34. Burr, B. Mapping and sequencing the rice genome. *Plant C.* **2002**, *14*, 521–523. [CrossRef]
35. The International Brachypodium Initiative. Genome sequence analysis of the model grass Brachypodium distachyon: Insights into grass genome evolution. *Nature* **2010**, *463*, 763–768. [CrossRef] [PubMed]
36. Filichkin, S.A.; Priest, H.D.; Givan, S.A. Genome-wide mapping of alternative splicing in Arabidopsis thaliana. *Genome Res.* **2010**, *20*, 45–58. [CrossRef]
37. Mallik, S.; Tawfik, D.S.; Levy, E.D. How gene duplication diversifies the landscape of protein oligomeric state and function. *Curr. Opin. Genet. Dev.* **2022**, *76*, 101966. [CrossRef] [PubMed]
38. Qiao, X.; Li, Q.; Yin, H.; Qi, K.; Li, L.; Wang, R.; Zhang, S.; Paterson, A.H. Gene duplication and evolution in recurring polyploidization-diploidization cycles in plants. *Genome Biol.* **2019**, *20*, 38. [CrossRef]
39. Guo, Z.H.; Ma, P.F.; Yang, G.Q.; Hu, J.Y.; Liu, Y.L.; Xia, E.H.; Zhong, M.C.; Zhao, L.; Sun, G.L.; Xu, Y.X. Genome Sequences Provide Insights into the Reticulate Origin and Unique Traits of Woody Bamboos. *Mol. Plant* **2019**, *12*, 1353–1365. [CrossRef]
40. Zhao, Y.; Su, X.; Wang, X.; Wang, M.; Cai, M. Comparative genomic analysis of TCP genes in six Rosaceae species and expression pattern analysis in Pyrus bretschneideri. *Front. Genet.* **2021**, *12*, 669959. [CrossRef]
41. Liebsch, D.; Palatnik, J.F. MicroRNA miR396, GRF transcription factors and GIF co-regulators: A conserved plant growth regulatory module with potential for breeding and biotechnology. *Curr. Opin. Plant Biol.* **2020**, *53*, 31–42. [CrossRef]
42. Cai, M.; Cheng, W.; Bai, Y.; Mu, C.; Zheng, H.; Cheng, Z.; Gao, J. PheGRF4e initiated auxin signaling during moso bamboo shoot development. *Mol. Biol. Rep.* **2022**, *49*, 8815–8825. [CrossRef] [PubMed]
43. Lantzouni, O.; Alkofer, A.; Falter-Braun, P.; Schwechheimer, C. GROWTH-REGULATING FACTORS Interact with DELLAs and Regulate Growth in Cold Stress. *Plant C.* **2020**, *32*, 1018–1034. [CrossRef] [PubMed]
44. Wei, Q.; Guo, L.; Jiao, C.; Fei, Z.; Chen, M.; Cao, J.; Ding, Y.; Yuan, Q. Characterization of the developmental dynamics of the elongation of a bamboo internode during the fast growth stage. *Tree Physiol.* **2019**, *39*, 1201–1214. [CrossRef]
45. Chen, M.; Guo, L.; Ramakrishnan, M.; Fei, Z.; Vinod, K.K.; Ding, Y.; Jiao, C.; Gao, Z.; Zha, R.; Wang, C.; et al. Rapid growth of Moso bamboo (Phyllostachys edulis): Cellular roadmaps, transcriptome dynamics, and environmental factors. *Plant C.* **2022**, *34*, 3577–3610. [CrossRef] [PubMed]
46. Chandran, V.; Wang, H.; Gao, F.; Cao, X.L.; Chen, Y.P.; Li, G.B.; Zhu, Y.; Yang, X.M.; Zhang, L.L.; Zhao, Z.X.; et al. miR396-OsGRFs module balances growth and rice blast disease-resistance. *Front. Plant Sci.* **2019**, *9*, 1999. [CrossRef]
47. Chen, Y.; Dan, Z.; Gao, F.; Chen, P.; Fan, F.; Li, S. Rice GROWTH-REGULATING FACTOR7 Modulates Plant Architecture through Regulating GA and Indole-3-Acetic Acid Metabolism. *Plant Physiol.* **2020**, *184*, 393–406. [CrossRef] [PubMed]
48. Tu, Z.; Xia, H.; Yang, L.; Zhai, X.; Shen, Y.; Li, H. The Roles of microRNA-Long Non-coding RNA-mRNA networks in the regulation of leaf and flower development in Liriodendron chinense. *Front. Plant Sci.* **2022**, *13*, 816875. [CrossRef]
49. Moison, M.; Pacheco, J.M.; Lucero, L.; Fonouni-Farde, C.; Rodríguez-Melo, J.; Mansilla, N.; Christ, A.; Bazin, J.; Benhamed, M.; Ibañez, F.; et al. The lncRNA APOLO interacts with the transcription factor WRKY42 to trigger root hair cell expansion in response to cold. *Mol. Plant.* **2021**, *14*, 937–948. [CrossRef]
50. Lu, Y.; Zeng, J.; Liu, Q. The Rice miR396-GRF-GIF-SWI/SNF Module: A Player in GA Signaling. *Front Plant Sci.* **2022**, *12*, 786641. [CrossRef]
51. Park, E.; Kim, Y.; Choi, G. Phytochrome B Requires PIF Degradation and Sequestration to Induce Light Responses across a Wide Range of Light Conditions. *Plant C.* **2018**, *30*, 1277–1292. [CrossRef]
52. Yan, C.; Yang, T.; Wang, B.; Yang, H.; Wang, J.; Yu, Q. Genome-Wide Identification of the WD40 Gene Family in Tomato (Solanum lycopersicum L.). *Genes* **2023**, *15*, 1273. [CrossRef] [PubMed]
53. Goodstein, D.M.; Shu, S.; Howson, R.; Neupane, R.; Hayes, R.D.; Fazo, J.; Mitros, T.; Dirks, W.; Hellsten, U.; Putnam, N.; et al. Phytozome: A comparative platform for green plant genomics. *Nucleic Acids Res.* **2012**, *40*, D1178–D1186. [CrossRef] [PubMed]
54. Larkin, M.A.; Blackshields, G.; Brown, N.P.; Chenna, R.; McGettigan, P.A.; McWilliam, H.; Valentin, F.; Wallace, I.M.; Wilm, A.; Lopez, R.; et al. Clustal W and Clustal X version 2.0. *Bioinformatics* **2007**, *23*, 2947–2948. [CrossRef] [PubMed]
55. Nguyen, L.T.; Schmidt, H.A.; von Haeseler, A.; Minh, B.Q. IQ-TREE: A fast and effective stochastic algorithm for estimating maximum-likelihood phylogenies. *Mol. Biol. Evol.* **2015**, *32*, 268–274. [CrossRef]
56. Campbell, K.; Gifford, R.J.; Singer, J.; Hill, V.; O'Toole, A.; Rambaut, A.; Hampson, K.; Brunker, K. Making genomic surveillance deliver: A lineage classification and nomenclature system to inform rabies elimination. *PLoS Pathog.* **2022**, *2*, e1010023. [CrossRef]
57. Hu, B.; Jin, J.; Guo, A.Y.; Zhang, H.; Luo, J.; Gao, G. GSDS 2.0: An upgraded gene feature visualization server. *Bioinformatics* **2015**, *31*, 1296–1297. [CrossRef]
58. Timothy, L.; Bailey James, J.; Charles, E.G.; William, S.N. The MEME Suite. *Nucleic Acids Res.* **2015**, *43*, W39–W49.
59. Wang, Y.; Tang, H.; Debarry, J.D.; Tan, X.; Li, J.; Wang, X.; Lee, T.H.; Jin, H.; Marler, B.; Guo, H.; et al. MCScanX: A toolkit for detection and evolutionary analysis of gene synteny and collinearity. *Nucleic Acids Res.* **2012**, *40*, e49. [CrossRef]
60. Liang, H.; Zhou, W.; Landweber, L.F. SWAKK: A web server for detecting positive selection in proteins using a sliding window substitution rate analysis. *Nucleic Acids Res.* **2016**, *34*, W382–W384. [CrossRef]
61. Krzywinski, M.; Schein, J.; Birol, I.; Connors, J.; Gascoyne, R.; Horsman, D.; Jones, S.J.; Marra, M.A. Circos: An information aesthetic for comparative genomics. *Genome Res.* **2009**, *19*, 1639–1645. [CrossRef]

62. Rozas, J.; Ferrer-Mata, A.; Sánchez-DelBarrio, J.C.; Guirao-Rico, S.; Librado, P.; Ramos-Onsins, S.E.; Sánchez-Gracia, A. DnaSP 6: DNA Sequence Polymorphism Analysis of Large Data Sets. *Mol. Biol. Evol.* **2017**, *34*, 3299–3302. [CrossRef] [PubMed]
63. Cao, J.; Huang, J.L.; Yang, Y.P.; Hu, X.Y. Analyses of the oligopeptide transporter gene family in poplar and grape. *BMC Genom.* **2011**, *12*, 465. [CrossRef]
64. Huang, Z.; Zhong, X.J.; He, J.; Jin, S.H.; Guo, H.D.; Yu, X.F.; Zhou, Y.J.; Li, X.; Ma, M.D.; Chen, Q.B.; et al. Genome-wide identification, characterization, and stress-responsive expression profiling of genes encoding LEA (Late Embryogenesis Abundant) proteins in Moso bamboo (Phyllostachys edulis). *PLoS ONE* **2016**, *11*, e0165953. [CrossRef] [PubMed]
65. Li, J.; Ma, W.; Zeng, P.; Wang, J.; Geng, B.; Yang, J.; Cui, Q. LncTar: A tool for predicting the RNA targets of long noncoding RNAs. *Brief Bioinform.* **2015**, *16*, 806–812. [CrossRef] [PubMed]
66. Addo-Quaye, C.; Miller, W.; Axtell, M.J. CleaveLand: A pipeline for using degradome data to find cleaved small RNA targets. *Bioinformatics* **2009**, *25*, 130–131. [CrossRef]
67. Zhang, Y. miRU: An automated plant miRNA target prediction server. *Nucleic Acids Res.* **2005**, *33*, W701–W704. [CrossRef]